Electronic Journal of Biotechnology 54 (2021) 1–7

Contents lists available at ScienceDirect

Electronic Journal of Biotechnology

journal homepage:

Research Article

Biogenic synthesis of selenium nanoparticles by *Shewanella* sp. HN-41 using a modified bioelectrochemical system

Cuong Tu Ho [a,*], Thi-Hanh Nguyen [b], Thuong-Thuong Lam [a], Dang-Quang Le [c], Canh Xuan Nguyen [d], Ji-hoon Lee [e], Hor-Gil Hur [f]

[a] *Institute of Environmental Technology, Vietnam Academy of Science and Technology, 18 Hoang Quoc Viet Str., Cau Giay Dist., Viet Nam*
[b] *Institute of Chemistry, Vietnam Academy of Science and Technology, 18 Hoang Quoc Viet Str., Cau Giay Dist., Viet Nam*
[c] *R&D Center of Bioactive Compounds, Vietnam Institute of Industrial Chemistry, No 2 Pham Ngu Lao, HoanKiem, Hanoi, Viet Nam*
[d] *Department of Biotechnology, Vietnam National University of Agriculture, Trau Quy, Hanoi, Viet Nam*
[e] *Department of Bioenvironmental Chemistry, Chonbuk National University, 567 Baekje-daero, Deokjin-gu, Jeonju-si, Jeollabuk-do, Republic of Korea*
[f] *School of Environmental and Earth Science, Gwangju Institute of Science and Technology, 123 Cheomdan gwagi-ro, Buk-gu, Gwangju 61005, Republic of Korea*

GRAPHICAL ABSTRACT

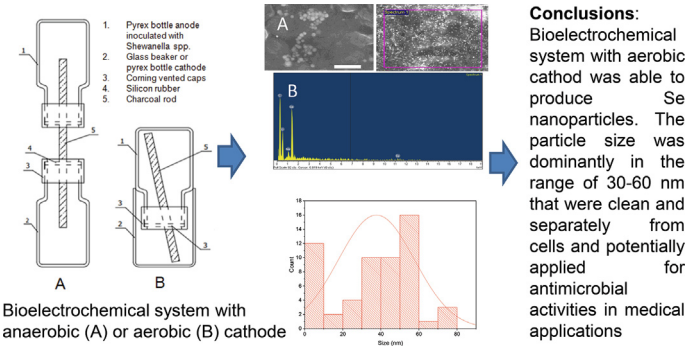

Bioelectrochemical system with anaerobic (A) or aerobic (B) cathode

Conclusions: Bioelectrochemical system with aerobic cathod was able to produce Se nanoparticles. The particle size was dominantly in the range of 30-60 nm that were clean and separately from cells and potentially applied for antimicrobial activities in medical applications

ARTICLE INFO

Article history:
Received 14 January 2021
Accepted 27 July 2021
Available online 4 August 2021

Keywords:
Anode
Bioelectrochemical system
Biogenic
Cathode
Nanoparticles
Nanosized selenium
Nonexternal circuit
Selenite
Selenium nanoparticles
Selenium
Shewanella sp.

ABSTRACT

Background: Synthesis of selenium nanoparticles from selenite by *Shewanella* sp. HN-41 demonstrated that particle size depended on the reaction time and biomass of cells. The slow reaction and low biomass tended to form small particles. In this study, *Shewanella* sp. HN-41 was introduced into the anode of a nonexternal circuit bioelectrochemical system (nec_BES) to convert chemical energy from lactate to low electron current to the cathode, where selenite was reduced.
Results: Our experiment with two systems, one bioelectrochemical system with a cathode flushed with nitrogen and the other with a no-nitrogen-flushing cathode, showed that the former could not produce Se nanoparticles after 21 d, but the latter formed them with an average size of 37.7 nm. The SEM and TEM images demonstrated that the particle size of 10 nm occupied over 10% and most of the particles were in the range of 30–60 nm. The XRD result and SAED image demonstrated no clear peaks of crystal and proved that the Se nanoparticles are amorphous.
Conclusions: The clean Se nanoparticles were synthesized and completely separated from bacterial cells in the bioelectrochemical system. This study opened a new approach for the biological synthesis of metal

Peer review under responsibility of Pontificia Universidad Católica de Valparaíso
* Corresponding author.
E-mail address: hotucuong@gmail.com (C.T. Ho).

https://doi.org/10.1016/j.ejbt.2021.07.004

nanoparticles. Finally, the Se products in the range of 30–60 nm can be tested for antimicrobial activities in medical applications.

How to cite: Ho CT, Nguyen T-H, Lam T-T, et al. Biogenic synthesis of selenium nanoparticles by *Shewanella* sp. HN-41 using a modified bioelectrochemical system. Electron J Biotechnol 2021;54. https://doi.org/10.1016/j.ejbt.2021.07.004

1. Introduction

Elemental selenium (Se) is a semisolid metal that belongs to Group 6 of the periodic table with an atomic number of 34; and its nanoparticles have been shown as a potential material in different fields including agricultural, biomedical, environmental, and industrial fields [1]. Se element played an important role in the industry because of its several important chemical and physical properties, including the following: a relatively low melting point (490 K), photovoltaic properties, high piezoelectricity, high photoconductivity (8104 S cm^{-1}), superconductivity, thermoelectric properties, linear and nonlinear optical properties, and high reactivity toward a variety of chemicals that are useful for the conversion of selenium into other functional materials [2]. Se nanoparticles were applied in the production of solar cells, rectifiers, photographic exposure meters, xerography, pigments, glasses, and steel. The biological function of Se nanoparticles has recently been reviewed thoroughly [1] and demonstrated that selenium nanoparticles could be applied as anticancer [3,4] and antioxidant [5], antibacterial, and antibiofilm [6] reagents. The remarkable antimicrobial activity of these nanoparticles has been tested in biomedical studies against pathogenic bacteria, fungi, and yeasts [7,8,9].

Stable manufacture of nanosized selenium materials has been achieved by many processes, including chemical, physical and biological processes. It was reported that selenium nanoparticles were synthesized by solvothermal, sonochemical, laser ablation, and microwave-enhanced reactions [10,11,12,13,14]. Many biological species are capable of reducing selenite and selenate [15,16,17]. Diverse selenium-respiring bacteria from various environments have been isolated and identified from selenite-contaminated agricultural drainage pond sediment, and deep ocean hydrothermal steam vents to plants that are capable of growing in selenite contaminating soils. Nanoparticles of selenium have been formed by diverse phylogenetic genera including *Rhizobiumselenireducens* sp., *Dechlorosoma* sp., *Pseudomonas* sp., *Sulfurospirilium* sp., *Desulfovibrio* sp., and *Shewanella* sp. [15,17,18,19]. Recently, biogenic routes for the formation of Se nanoparticles have been found in green chemistry in which plants [3], flower broth [20], and fruit juice [9] have been used. However, those chemical, physical, and biological methods for the syntheses of selenium nanoparticles posed several limiting factors. The chemical and physical methods were probably costly and environmentally harmful. The biological route provided a cost-effective method, but the produced nanoparticles were difficult or costly to remove from cells.

Recently, new platform biotechnology, bioelectrochemical system (BES), has been investigated to employ microorganisms to convert the chemical energy from organic materials to electric current. A BES consists of an optional separator and two compartments; one is the anode containing the medium and microbes for electron generation, and the other is the cathode containing solution flushed with oxygen (or other oxidizers) as electron acceptor. BES configuration has been investigated to improve energy efficiency and its applications. In the BES, the chemical energy from organic matter is converted to generate electron flow from anode to cathode through an external circuit, wherein the cathode chamber, the electrons can be used for direct electricity production (microbial fuel cells, MFCs), or the reduction of water or oxidized chemicals, such as metal ions, CO_2, or organic chemicals (microbial electrolysis cells, MECs, or microbial electro-synthesis, MES) [21,22,23]. Most of the BES configurations were attempted to overcome the internal resistance and increase the electron current. However, the application of BESs with low power and continuous and low electron current has not yet been exploited.

In this study, the synthesis of Se nanoparticles was investigated in the nonexternal circuit bioelectrochemical system (*nec*_BES) to separate the particles from cells and biological substances, for further applications. Conventionally, MFC includes an external electrical circuit by the copper wire connecting the cathode and anode, and proton exchanged from anode to cathode, through an ion-exchange membrane. In our study, the *nec*_BES without both external electrical circuit and ion exchange membrane were applied for the synthesis of Se nanoparticles. The *Shewanella* sp., HN-41 cells were inoculated into the anode with the lactate substrates, the cells were hypothesized to donate low electron current to one graphite electrode (that connects anode and cathode directly without the external circuit of copper wire), and then, the low electron current reduced selenite directly or indirectly into selenium. The products in the cathode were collected and characterized by SEM, TEM, SAED, and XRD.

2. Materials and method

2.1. nec_BES construction

Two types of *nec*_BESs were designed; both included two separate anodic and cathodic chambers that were directly connected to each other by the charcoal rod of the electrode perforating through the silicon membrane. The two types of *nec*_BESs were different from each other in the cathodic chamber condition. One type had a cathodic chamber bubbled with nitrogen to remove oxygen and the other was bubbled neither with nitrogen nor oxygen to maintain atmospheric oxygen condition in the cathodic chamber (Fig. 1).

2.2. Preparation for the anode chamber

The anodic chambers were filled with 100 ml of sterilized mineral medium and bubbled with filtered nitrogen gas in a clean bench for 5 min, as reported previously, to maintain the dissolved oxygen level at 0.24 mg/L [18]. The fresh cells of *Shewanella* sp., *HN-41* cultured in the LB agar medium were harvested after two days of incubation at room temperature, and inoculated into the anodic chamber by injecting 1 ml of fresh cells suspended in sterilized sodium chloride solution (0.9%). Then, the filtered sodium lactate was added into the anodic chamber at the final concentration of 10 mM by a 1 ml sterilized syringe.

The mineral media were prepared with distilled water which was bubbled with nitrogen using the following components (g/L): $NaHCO_3$: 2.5, $CaCl_2$: 0.06, NH_4Cl: 1, $MgCl_2{\cdot}H_2O$: 0.2, KCl: 0.1, beta-glycerophosphoric acid disodium salt: 0.06, NaCl: 10, HEPES (N-(2-hydroxyethyl)piperazine-N′-2-ethanesulphonic acid): 7.2, yeast extract: 0.1, and 10 ml of mineral micronutrients

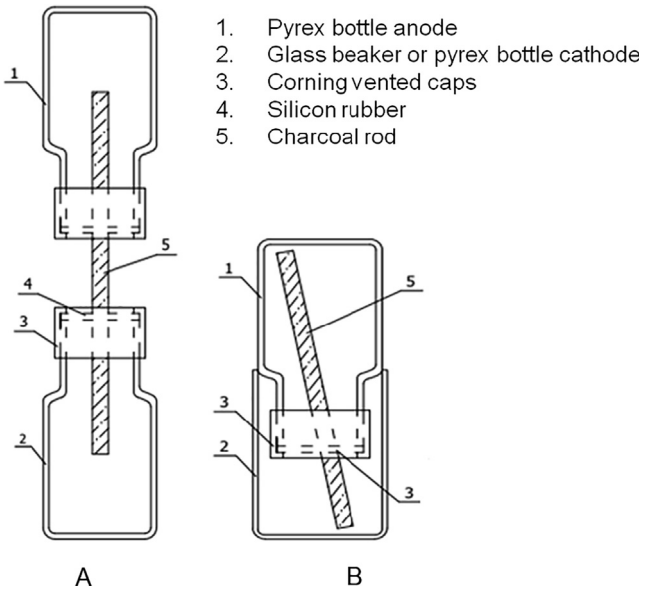

Fig. 1. The configuration for the *nec*_BES with the anaerobic (A) and aerobic (B) cathode.

including nitriloacetic acid, $FeCl_2$, Na_2WO_4, $MnCl_2$, $CoCl_2$, $ZnCl_2$, $CuCl_2$, boric acid, Na_2MoO_4, Na_2SeO_3, and $NiCl_2$. The pH of the media solution was adjusted to pH 7.6 using 10 N NaOH solution as prepared in the previous report [24]. All chemicals were purchased from Fisher Scientific (Loughborough, UK) or Merck (Damstadt, Germany) and *Shewanella* sp., HN-41 cells were provided by the Lab of Applied and Environmental Microbiology, School of Earth Science and Environmental Engineering, Gwangju Institute of Science and Technology.

2.3. Preparation of the cathodic chambers

1) For the anaerobic cathodic chamber, 1 mM Selenite solution was used as catholyte and added into the cathodic chamber (silicon rubber –capturing Pyrex bottle (Fig. 1). Then the anaerobic cathode was bubbled with purified nitrogen gas for 5 min to remove the air and oxygen in the catholyte, and the dissolved oxygen level reached 0.24 mg/L [18].
2) For the aerobic cathodic chamber, 1 mM Selenite solution was also used as catholyte and added into the cathodic chamber without bubbling nitrogen (glass beaker (Fig. 1)).

All the catholytes were prepared with distilled and deionized water.

The control experiment was prepared as in the *nec*_BES with aerobic cathode, except for the anodic chamber. The anode of the control *nec*_BES was not inoculated with fresh cells but was added with sodium lactate at the final concentration of 10 mM.

2.4. Operation and sampling of nec_BESs

All sampling and monitoring of solutions were performed at both cathode and anode chambers. The cathodic solutions were sampled at days 0, 2, 4, 6, 14, and 21 for selenite concentration. The anodic solutions were sampled at days 0, 2, 4, and 6 for the lactate. For monitoring of the cell growth, 2 ml of anodic solution were measured at the wavelength of 600 nm for optical density and the pH of anodic solutions was monitored at days 0, 2, 4, 6, 14, and 21. The lactate was continuously added to the final concentration of 10 mM after 7 d of incubation to provide the substrate sources with bacterial cells. The products in the cathode were collected on day 21 and washed with distilled water twice by centrifugation at 12 000 rpm for 5 min. Collected products were characterized by SEM, TEM, and XRD.

2.5. Analysis of the samples and products

The anodic samples (1 mL) were filtered through a 0.2 μm Whatman syringe filter (GE Healthcare, UK). Ten microliters of the filtrate were injected into the high-performance liquid chromatography (HPLC), which was equipped with a photodiode array (PDA) detector (Varian, Walnut Creek, CA) and an Aminex HPX-87H ion exclusion column (Bio-Rad, Hercules, CA) for the quantification of lactate. The HPLC was run in the isocratic flow mode at the flow rate of 0.6 mL min^{-1} for 30 min and the mobile phase of 5 mM sulfuric acid. The lactate was detected at 210 nm with the UV detector. The concentration of lactate was calculated based on the standard curve of lactate in the same condition of the mobile phase.

Selenite concentration in the cathode was analyzed by atomic absorption spectrometry (AAS) method on a Perkin Elmer 3300 instrument (Perkin Elmer, Shelton, CT). Briefly, 1 ml of cathodic sample was centrifuged at 12 000 rpm and the supernatant of the sample was injected into the AAS. The concentration of selenite was calculated based on the prepared standard curve of selenite in the AAS.

The washed samples of cathode products were analyzed by EDS, SEM, TEM, and XRD. SEM images were recorded with a Hitachi S4800 (Japan). The samples (100 μL) were dropped and dried on a carbon tape in a specimen holder. Energy dispersive X-ray spectroscopy (EDS) was also performed to analyze the elemental composition of the samples. For TEM analysis, ten microliters of the washed sample were dropped on the copper grid and dried at room temperature. TEM images were obtained at JEOL JEM-1010 (Tokyo, Japan) and HR-TEM images were obtained using a JEM-2100 (Tokyo, Japan). The particles size was calculated based on the analysis of the TEM image using the software ImageJ. For XRD analysis, the measurement was conducted by using a *D*/max Ultima III diffractometer (Rigaku, Tokyo, Japan), equipped with monochromatic high-intensity Cu Ka radiation (λ = 1.5406 Å).

3. Results

3.1. Selenium nanoparticles syntheses in the cathode

In our investigation, the color of the cathodic solution changed from colorless to pinkish in the *nec*_BES with aerobic cathode, after 21 d of incubation at room temperature. The cathodic solution was centrifuged to collect the precipitant and the washed precipitant was observed at SEM (Fig. 2) and TEM (Fig. 3). The SEM image described clear spherical nanoparticles formed from the aerobic cathodic solution of *nec*_BES. The EDS data showed the peak of the Se element in the SEM image (Fig. 2B), confirming that the precipitant was selenium. For the samples from the anaerobic cathode, the cathodic solution did not show the change of color and the particles were not observed by SEM images (data not shown).

The collected Se products were mounted for XRD analysis. The data obtained showed no major peak of crystals Fig. 4). Further analysis by TEM showed that the precipitant was spherical with a size range from several nanometers to 80 nm, with an average size of 37.7 nm (Fig. 3). The size of the particle was distributed into two main groups under 10 nm and around 50 nm (Fig. 3B). The small dot of selenium nanoparticles is depicted in Fig. 4A along with the aggregate of large particles. The inserted image of a selected area electron diffraction image showed the reflection of an electron beam with a large hollow hole at the center without the ring of an electron beam, confirming that the crystallinity of Se particles was amorphous.

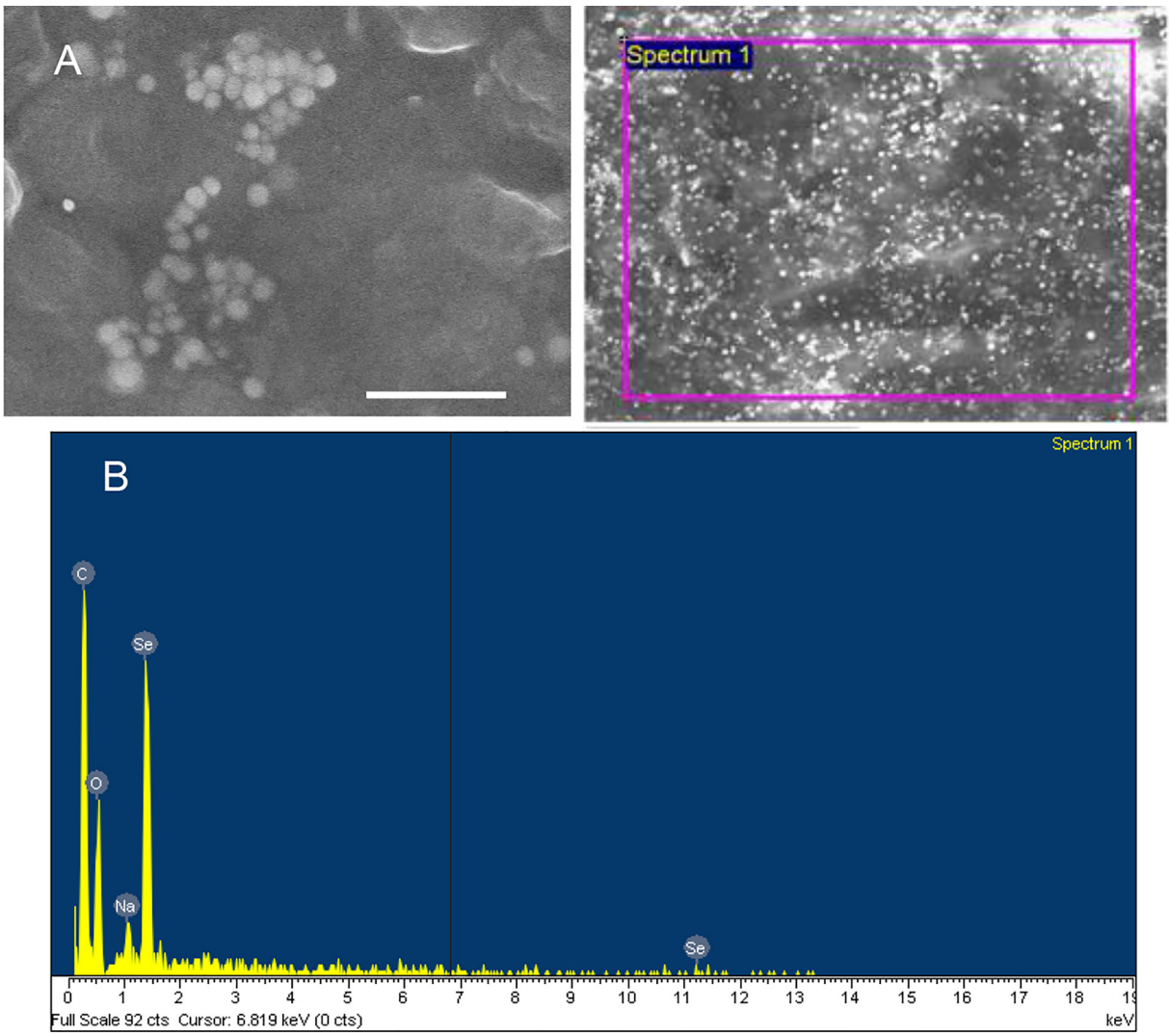

Fig. 2. SEM (A) images and EDS (B) data of Se(0) nanoparticles formed in the aerobic cathode of the *nec*_BES inoculated with *Shewanella* sp. HN-41, scale bar of 500 nm.

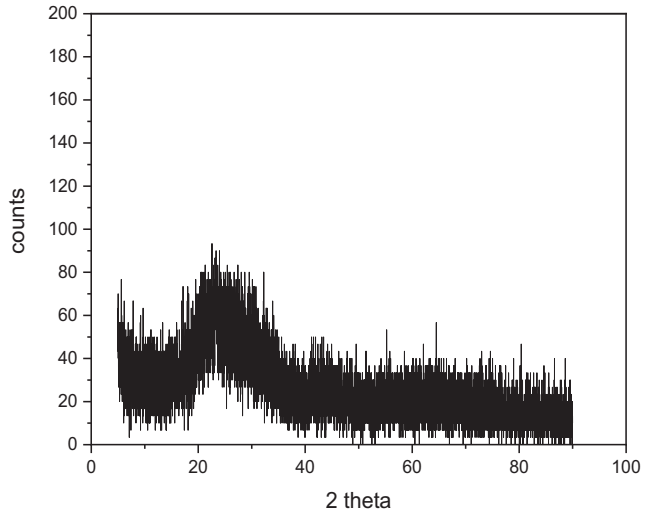

Fig. 3. XRD pattern of the Se nanoparticles produced in the cathodic solution.

The selenite concentration in the aqueous solution of the cathode was monitored to observe the reduction of selenite. The results of the AAS analysis demonstrated that the selenite at the aerobic cathode was reduced, but not at the anaerobic cathode (Fig. 5). The rate of selenite reduction was slow in the *nec*_BES with an aerobic cathode. The selenite concentration at the aerobic cathode reduced approximately about 6% after 21 incubation days, whereas, the negligible amount of selenite (0.7%) in the anaerobic cathode was lost. In the control, the concentration of selenite at the cathode changed about 1.1% (Fig. 5), which is the amount of the CCV sample (1.5%, data not shown).

3.2. Variation of cell, pH, and substrate in the anode

The reaction in the anode is observed as given in Fig. 6, describing the consumption of lactate substrate in both types of *nec*_BESs. The lactate concentration decreased from 10 mM to 6 and 1 mM in the *nec*_BES with aerobic cathode after 2 and 4 d, respectively. In the *nec*_BES with an anaerobic cathode, the rate of lactate consumption was slower and the lactate concentration reduced from 10 mM to c.a. 6 mM on the fourth day. In the control without *Shewanella* cells, the lactate concentration did not change from day 0 to 6. On the sixth day, the lactate was not observed in both types of *nec*_BESs by HPLC, confirming that bacterial cells consumed all the substrates, and thereby, the lactate was added into the anodes up to 10 mM after every six days to supplement the substrate for the cells.

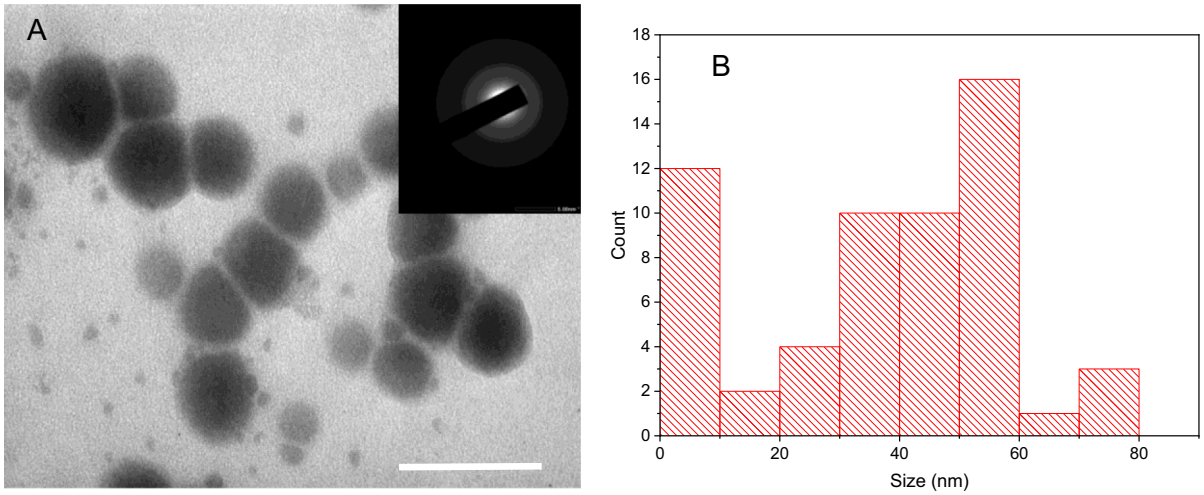

Fig. 4. TEM (A) image and size distribution (B) of the Se(0) nanoparticles formed in the aerobic cathode of the *nec*_BES inoculated with *Shewanella* sp. HN4, inserted image SAED of a Se particle, scale bar of 100 nm.

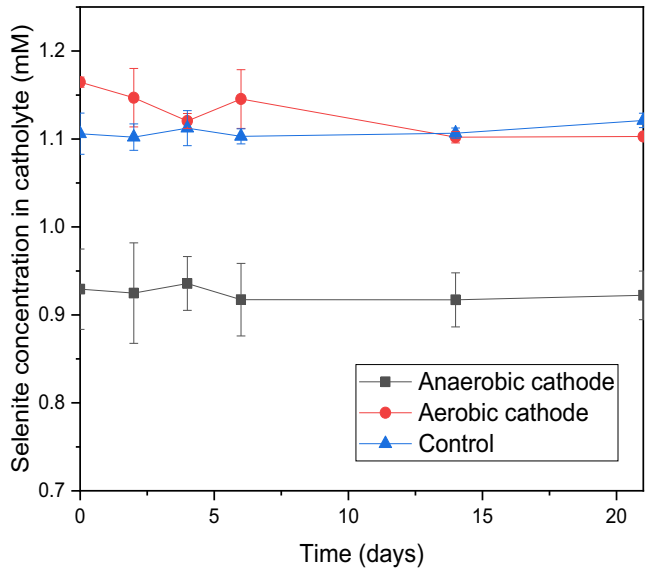

Fig. 5. Selenite concentration in the aqueous phase of the cathode solution of different *nec*_BESs.

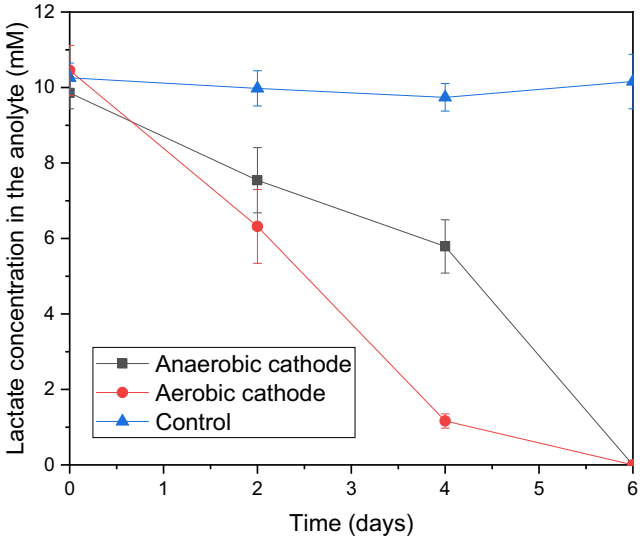

Fig. 6. Lactate concentration in the filtered aqueous medium from the anode of different *nec*_BESs.

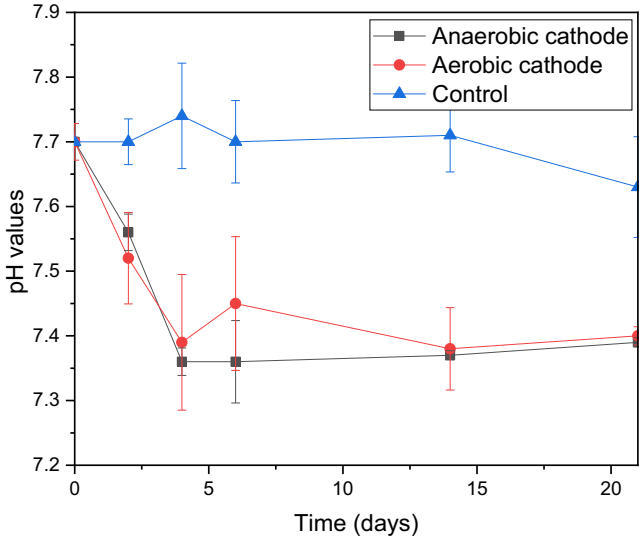

Fig. 7. pH values of the aqueous medium from the anode of different *nec*_BESs.

In addition to lactate reduction, the pH of the medium in the anode of both *nec*_BESs was changed from 7.7 to 7.5 after two days of incubation (Fig. 7). Then the pH remained stable at 7.4 in both *nec*_BESs, and pH in the control *nec*_BES was stable at approximately 7.7 from day 0 to 21. It indirectly confirmed that bacterial cells consumed the lactate and produced an acidic environment in the anode.

In this study, the growth of bacterial cells was measured through the optical density of cells at the wavelength of 600 nm in UV–VIS spectrometry. The result in Fig. 8 showed no increase in the OD of cells in both experimental anodes of *nec*_BESs. However, at the end of the experiment, the silicon membranes of the anodes were observed with a layer of pink-colored cells, forming a biofilm in the silicon membranes (Fig. S1).

4. Discussion

4.1. BES current with single strain Shewanella

BESs, typically microbial fuel cells (MFCs), uses current-generating microorganisms as biocatalysts to convert organic sub-

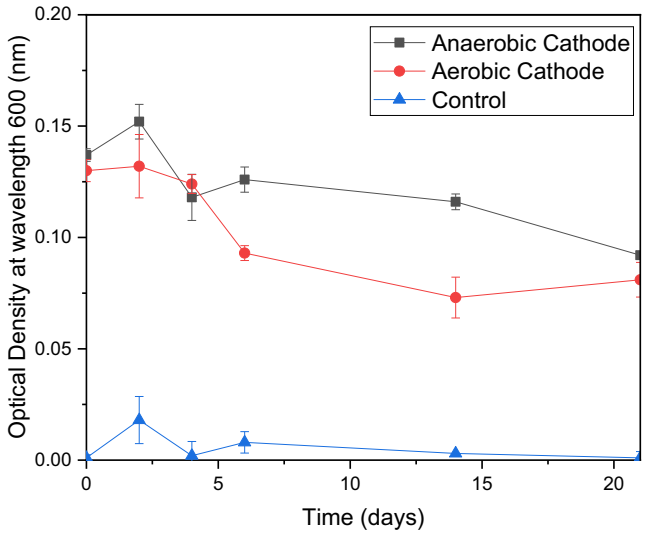

Fig. 8. The optical density of suspended cells in the aqueous medium from the anode of different *nec*_BESs.

stances into electricity [25]. These microorganisms include members of the *Geobacter* family, *Shewanella putrefaciens* and *Shewanella oneidensis*, *Rhodoferax ferrireducens*, *Pseudomonas aeruginosa*, *Clostridium butyrium*, and *Aeromonas hydrophila*— that have been reported to oxidize organic matter at the anode to complete their metabolism process [26]. Among these bacteria, *Shewanella* and *Geobacter* genera are the most frequently used model organisms in the studies of BESs. Whereas, many MFCs operations were reported with *Shewanella* sp. as a model organism [27,28], which is a facultative anaerobic bacteria [29]. In this study, the cells of anaerobically grown *Shewanella* sp., HN-41 are electrochemically active and can use lactate as an electron donor source as in stoichiometric Equation 1 and donate the electron to its terminal electron acceptor [18,24,30].

In our system, the electron and proton produced were donated to the electrode of the anode and HEPES buffer, respectively. The pH of the *nec*_BES anode was decreased and stabilized at pH 7.4 as a consequence of the lactate oxidation to release H^+ and buffering of HEPES in the medium. The electron current could not be measured because of the difficult setup of our bottle configuration, where the graphite electrode worked as an electron wire to the terminal electron acceptor in the cathode. A previous study [31] with different bottle configurations of MFC showed that *Shewanella oneidensis* MR1 single-strain MFC showed higher internal resistance and lower maximum power density than MFC with mixed cultures in all configurations. It also reported that the MFC with a higher number of bottles had higher internal resistance and lower power density.

$$CH_3CH_2OCOO^- + H_2O \rightarrow CH_3COO^- + CO_2\uparrow + 4e + 4H^+ \quad \text{Equation1}$$

The anode performance in *Shewanella* inoculated MFC is influenced largely by such factors as anolyte pH, inoculum age, the concentration of electron donor, calcium chloride, and riboflavin [27,32]. *Shewanella* sp. were reported to secrete riboflavin that facilitates electron transfer to both insoluble metals and anodes. The removal of accumulated soluble flavins decreases the rate of electron transfer by *Shewanella* biofilm to electrodes over 70% [33]. In this study, we have controlled only the first three parameters, but not calcium chloride and riboflavin, to reduce the electron current to cathode. This hypothesizes that slow reaction will result in small-sized Se nanoparticles [24]. The HEPES buffer maintained pH stable until 21 d of the experiment, although the oxidation of lactate continuously released protons during the experiment.

4.2. Chemical reaction and selenium nanoparticle formation in the cathode

The fact that the lactate was consumed and pH dropped in the anode in both *nec*_BESs but no Se nanoparticles were formed (or no selenite reduction occurred) in the anaerobic cathode of *nec*_BESs, can be explained by the configuration of air–cathode. The single-chamber MFC with an air-carbon electrode with/without proton exchange membrane (PEM) was able to transfer electrons to dissolved oxygen and generate the electron current [34]. In our *nec*_BESs, there was an air gap between two chambers; thereby, the electron from the anode probably got transferred to dissolved oxygen from the air at the air-open end of the electrode. The difference between the two types of *nec*_BESs was that there exited dissolved oxygen in the aerobic cathode, which acted as an electron acceptor in the aerobic cathode. As the redox potential of the Se(IV)/Se(0) couple is −0.366 V (vs SHE at 25°C) in Equation 2 [35,36], oxygen/H_2O couple with redox potential of +1.22 V (vs SHE at 25°C) in Equation 3 [36,37] will be preferred to selenite as terminal electron acceptor. The dissolved oxygen was hypothesized to act as electron withdrawer to the cathode; thereby, the electron current was possible to reduce both selenites according to Equation 2 and oxygen according to Equation 3, competitively. The reaction of selenite reduction into selenium (Se nanoparticle) that occurs at a slow rate in our experiment, may be because of the competitiveness of the two chemicals. The important role of oxygen in the cathode reaction as a terminal electron acceptor was observed in the study of selenite removal in a single-chamber air–cathode MFC [38].

$$SeO_3^{2-} + 3H_2O + 4e^- \leftrightarrow Se + 6OH^- \ -0.366\ V \quad \text{Equation2}$$

$$O_{2(g)} + 4H^+_{(aq)} + 4e^- \leftrightarrow 2H_2O \ +1.22\ V \quad \text{Equation3}$$

Selenium possesses multiple oxidation states and can engage in numerous self-exchange reactions: Se(VI)/Se(IV), Se(IV)/Se(0), Se(IV)/Se(-II), and Se(0)/Se(-II). In this study, selenite was used as an electrolyte in the cathode and could be reduced to Se(0) and Se(-II). Previous voltammetric studies of Se have shown that two steps of the selenite reduction included the first one from Se(IV) to Se(0) and the second one from Se(0) to Se(-II) scheme, where the reduction of Se(0) took place at the more negative potentials [36]. The species Se(-II) exists at lower than −0.7 V and Se(0) occurs in the range of −0.4 to 0.3 V at pH 6 ~ 8 based on the potential–pH equilibrium diagram for the system selenium–water, at 25°C [35]. Therefore, the species Se(-II) could not exist in the solution, because the reduction potential at the cathode after the experiment was approximately 0.15 (V) at pH 7.

Amorphous selenium nanoparticles formed in the cathodic solution were similar to that of other studies [2,18,24]. The cathodic solution contained only ions, dissolved oxygen, and water as a solvent; it lacked catalysts for the crystallization process of selenium. Ho et al. [38] suggested applying the DMSO as a solvent for the crystallization of Se produced *Shewanella* spp. It also suggested that there was a clear relationship between the type of crystal grown and the dielectric constants of the solvents [39]. Crystal selenium was also formed in the environment with stabilized chemicals and reducing agents [3,40]. In this study, benign environment conditions were applied; therefore, the amorphous Se nanoparticles were formed slowly with small-sized particles.

5. Conclusions

The successful synthesis of Se nanoparticles from selenite by *nec*_BES has proposed a new method for the formation of Se nanoparticles, in which the particle size is smaller and completely separated from the biological cells and materials. In this study, the *Shewanella* sp., HN-41 was introduced in the anode of *nec*_BES to

use the substrate and generate a low electron current to the cathode. The clean and amorphous Se(0) nanoparticles formed with an average size of 37.7 nm in our experiment after 21 d, were expected to have better application in the material and biomedical sciences. The configuration of *nec*_BES allowed to extract energy from organic matters such as organic wastes for the synthesis of Se nanoparticles in the other clean medium at the cathode, implying the combination of wastewater treatment and Se(0) synthesis. Finally, the independent solution in the cathode can be modified for the synthesis of stable and functional Se nanoparticles that can be tested for antimicrobial activities in the future.

Financial support

This research is funded by Vietnam National Foundation for Science and Technology Development (NAFOSTED) under grant number: 104.03-2016.45.

Conflict of interest

There is no conflict of interest for this article.

Supplementary material

https://doi.org/10.1016/j.ejbt.2021.07.004.

Data availability

All the data are available in the personal storage in google drive. The link can be found here: https://drive.google.com/drive/folders/1umTBNPrlIDmLtS5PiUKOKTisaFDT4MBc. If there is anything concerned with the data, please contact the email hotucuong@gmail.com.

References

[1] Nayak V, Singh KR, Singh AK, et al. Potentialities of selenium nanoparticles in biomedical science. New J Chem 2021;45:2849–78. https://doi.org/10.1039/D0NJ05884J.
[2] Tam K, Ho CT, Lee J-H, et al. Growth mechanism of amorphous selenium nanoparticles synthesized by *Shewanella* sp. HN-41. Biosci Biotechnol Biochem 2010;74:696–700. https://doi.org/10.1271/bbb.90454. PMid: 20378977.
[3] Anu K, Devanesan S, Prasanth R, et al. Biogenesis of selenium nanoparticles and their anti-leukemia activity. J King Saud Univ - Sci 2020;32:2520–6. https://doi.org/10.1016/j.jksus.2020.04.018.
[4] Yu B, Zhang Y, Zheng W, et al. Positive surface charge enhances selective cellular uptake and anticancer efficacy of selenium nanoparticles. Inorg Chem 2012;51:8956–63. https://doi.org/10.1021/ic301050v. PMid: 22873404.
[5] Forootanfar H, Adeli-Sardou M, Nikkhoo M, et al. Antioxidant and cytotoxic effect of biologically synthesized selenium nanoparticles in comparison to selenium dioxide. J Trace Elem Med Biol 2014;28:75–9. https://doi.org/10.1016/j.jtemb.2013.07.005. PMid: 24074651.
[6] Shakibaie M, Forootanfar H, Golkari Y, et al. Anti-biofilm activity of biogenic selenium nanoparticles and selenium dioxide against clinical isolates of *Staphylococcus aureus*, *Pseudomonas aeruginosa*, and *Proteus mirabilis*. J Trace Elem Med Biol 2015;29:235–41. https://doi.org/10.1016/j.jtemb.2014.07.020. PMid: 25175509.
[7] Nguyen THD, Vardhanabhuti B, Lin M, et al. Antibacterial properties of selenium nanoparticles and their toxicity to Caco-2 cells. Food Control 2017;77:17–24. https://doi.org/10.1016/j.foodcont.2017.01.018.
[8] Vahdati M, Tohidi MT. Synthesis and characterization of selenium nanoparticles-lysozyme nanohybrid system with synergistic antibacterial properties. Sci Rep 2020;10:1–10. https://doi.org/10.1038/s41598-019-57333-7. PMid: 31949299.
[9] Alvi GB, Iqbal MS, Ghaith MMS, et al. Biogenic selenium nanoparticles (SeNPs) from citrus fruit have anti-bacterial activities. Sci Rep 2021;11:4811. https://doi.org/10.1038/s41598-021-84099-8. PMid: 33637796.
[10] Lin Z, Wang CRC. Evidence on the size-dependent absorption spectral evolution of selenium nanoparticles. Mater Chem Phys 2005;92:591–4. https://doi.org/10.1016/j.matchemphys.2005.02.023.
[11] Li X, Li Y, Li S, et al. Single crystalline trigonal selenium nanotubes and nanowires synthesized by sonochemical process. Cryst Growth Des 2005;5:911–6. https://doi.org/10.1021/cg049681q.
[12] Gao BX, Zhang J, Zhang L. Hollow sphere Selenium nanoparticles: their in-vitro anti hydroxyl radical effect. Adv Mater 2002;14:2000–3. https://doi.org/10.1002/1521-4095(20020219)14:4<290::AID-ADMA290>3.0.CO;2-U.
[13] Quintana M, Haro-Poniatowski E, Morales J, et al. Synthesis of selenium nanoparticles by pulsed laser ablation. Appl Surf Sci 2002;195:175–86. https://doi.org/10.1016/S0169-4332(02)00549-4.
[14] Zhang S, Liu Y, Ma X, et al. Rapid, large-scale synthesis and electrochemical behavior of faceted single-crystalline selenium nanotubes. J Phys Chem B 2006;110:9041–7. https://doi.org/10.1021/jp056718o. PMid: 16671713.
[15] Oremland RS, Herbel MJ, Blum JS, et al. Structural and spectral features of selenium nanospheres produced by Se-respiring bacteria. Appl Environ Microbiol 2004;70:52–60. https://doi.org/10.1128/AEM.70.1.52-60.2004. PMid: 14711625.
[16] Abdelouas A, Gong WL, Lutze W, et al. Using cytochrome c3 to make selenium nanowires. Chem Mater 2000;12:1510–2. https://doi.org/10.1021/cm990763p.
[17] Tomei FA, Barton LL, Lemanski CL, et al. Transformation of selenate and selenite to elemental selenium by *Desulfovibrio desulfuricans*. J Ind Microbiol 1995;14:329–36. https://doi.org/10.1007/BF01569947.
[18] Lee J-H, Han J, Choi H, et al. Effects of temperature and dissolved oxygen on Se (IV) removal and Se(0) precipitation by *Shewanella* sp. HN-41. Chemosphere 2007;68:1898–905. https://doi.org/10.1016/j.chemosphere.2007.02.062. PMid: 17434567.
[19] Li D-B, Cheng Y-Y, Wu C, et al. Selenite reduction by *Shewanella oneidensis* MR-1 is mediated by fumarate reductase in periplasm. Sci Rep 2015;4:3735. https://doi.org/10.1038/srep03735. PMid: 24435070.
[20] Deepa B, Ganesan V. Biogenic synthesis and characterization of selenium nanoparticles using the flower of *Bougainvillea spectabilis* Willd.. Int J Sci Res 2013;4:690–5.
[21] Choi C, Cui Y. Recovery of silver from wastewater coupled with power generation using a microbial fuel cell. Bioresour Technol 2012;107:522–5. https://doi.org/10.1016/j.biortech.2011.12.058. PMid: 22217729.
[22] Logan BE. Scaling up microbial fuel cells and other bioelectrochemical systems. Appl Microbiol Biotechnol 2010;85:1665–71. https://doi.org/10.1007/s00253-009-2378-9. PMid: 20013119.
[23] Wang H, Ren ZJ. Bioelectrochemical metal recovery from wastewater: A review. Water Res 2014;66:219–32. https://doi.org/10.1016/j.watres.2014.08.013. PMid: 25216302.
[24] Yang Y, Xu M, Guo J, et al. Bacterial extracellular electron transfer in bioelectrochemical systems. Process Biochem 2012;47:1707–14. https://doi.org/10.1016/j.procbio.2012.07.032.
[25] Logan BE, Regan JM. Electricity-producing bacterial communities in microbial fuel cells. Trends Microbiol 2006;14:512–8. https://doi.org/10.1016/j.tim.2006.10.003. PMid: 17049240.
[26] Kim HJ, Park HS, Hyun MS, et al. A mediator-less microbial fuel cell using a metal reducing bacterium, *Shewanella putrefaciens*. Enzyme Microb Technol 2002;30:145–52. https://doi.org/10.1016/S0141-0229(01)00478-1.
[27] Sharma V, Kundu PP. Biocatalysts in microbial fuel cells. Enzyme Microb Technol 2010;47:179–88. https://doi.org/10.1016/j.enzmictec.2010.07.001.
[28] Lovley DR, Holmes DE, Nevin KP. Dissimilatory Fe(III) and Mn(IV) reduction. Adv Microb Physiol 2004;49:219–86. https://doi.org/10.1016/S0065-2911(04)49005-5.
[29] Lee J, Roh Y. Microbial production and characterization of superparamagnetic magnetite nanoparticles by *Shewanella* sp. HN-41. J Microbiol Biotechnol 2008;18:1572–7.
[30] Watson VJ, Logan BE. Power production in MFCs inoculated with *Shewanella oneidensis* MR-1 or mixed cultures. Biotechnol Bioeng 2010;105:489–98. https://doi.org/10.1002/bit.22556. PMid: 19787640.
[31] Park. D, Zeikus J. Impact of electrode composition on electricity generation in a single-compartment fuel cell using *Shewanella putrefaciens*. Appl Microbiol Biotechnol 2002;59:58–61. https://doi.org/10.1007/s00253-002-0972-1. PMid: 12073132.
[32] Marsili E, Baron DB, Shikhare ID, et al. *Shewanella* secretes flavins that mediate extracellular electron transfer. Proc Natl Acad Sci U S A 2008;105:3968–73. https://doi.org/10.1073/pnas.0710525105. PMid: 18316736.
[33] Liu H, Logan BE. Electricity generation using an air-cathode single chamber microbial fuel cell in the presence and absence of a proton exchange membrane. Environ Sci Technol 2004;38:4040–6. https://doi.org/10.1021/es0499344. PMid: 15298217.
[34] Bouroushian M. Electrochemistry of the chalcogens. In: Electrochemistry of metal chalcogenides. Monographs in electrochemistry. Berlin, Heidelberg: Springer; 2010. p. 57–75. https://doi.org/10.1007/978-3-642-03967-6_2.
[35] Saji VS, Lee C-W. Selenium electrochemistry. RSC Adv 2013;3(26):10058. https://doi.org/10.1039/c3ra40678d.
[36] Anderson AB. Insights into electrocatalysis. Phys Chem Chem Phys 2012;14:1330–8. https://doi.org/10.1039/C2CP23616H. PMid: 22159903.
[37] Catal T, Bermek H, Liu H. Removal of selenite from wastewater using microbial fuel cells. Biotechnol Lett 2009;31:1211–6. https://doi.org/10.1007/s10529-009-9990-8. PMid: 19343501.
[38] Ho CT, Kim JW, Kim WB, et al. Shewanella-mediated synthesis of selenium nanowires and nanoribbons. J Mater Chem 2010;20:5899. https://doi.org/10.1039/b923252d.
[39] Ohtani T, Takayama N, Ikeda K, et al. Unusual crystallization behavior of selenium in the presence of organic molecules at room temperature. Chem Lett 2004;33:100–1. https://doi.org/10.1246/cl.2004.100.
[40] Gangadoo S, Stanley D, Hughes RJ, et al. The synthesis and characterisation of highly stable and reproducible selenium nanoparticles. Inorg Nano-Metal Chem 2017;47:1568–76. https://doi.org/10.1080/24701556.2017.1357611.